

## Identification of the Molecular Precursors for Hydrazine Solution Processed CuIn(Se,S)<sub>2</sub> Films and Their Interactions

Choong-Heui Chung, Sheng-Han Li, Bao Lei, Wenbing Yang, William W. Hou, Brion Bob, and Yang Yang\*

Department of Materials Science and Engineering, University of California Los Angeles, Los Angeles, California 90095, United States

Received November 12, 2010. Revised Manuscript Received December 21, 2010

We investigate the molecular species present in hydrazine CuIn(Se,S)<sub>2</sub> precursor solutions, their interactions, and phase formation in solution processed CuIn(Se,S)<sub>2</sub> thin films through Raman spectroscopy. The reaction between Cu<sub>2</sub>S and sulfur yields [Cu<sub>6</sub>S<sub>4</sub>]<sup>2-</sup> ions, while [In<sub>2</sub>Se<sub>4</sub>]<sup>2-</sup> ions are formed by the reaction of In<sub>2</sub>Se<sub>3</sub> with selenium within their respective solutions. Once combined to prepare a CuIn(Se,S)<sub>2</sub> precursor solution, these two species appear to be bridged via newly formed In–S bonds. The creation of the In–S bonds in the CuIn(Se,S)<sub>2</sub> precursor solution provides strong evidence for the mixing of copper, indium, sulfur, and selenium at a molecular level even prior to deposition. From this configuration, relatively little atomic diffusion is required to reach the chalcopyrite structure, which enables the formation of highly uniform polycrystalline CuIn(Se,S)<sub>2</sub> films at relatively low temperatures.

### Introduction

The use of high vacuum deposition techniques in the preparation of CuInSe<sub>2</sub> and related chalcopyrites has allowed researchers to fabricate laboratory-scale thin film solar cells with efficiencies approaching 20%.<sup>1</sup> However, vacuum processing presents a number of challenging issues that must be addressed before the production of low cost and large area photovoltaic modules can be fully realized.<sup>2,3</sup> Nonvacuum deposition techniques offer an important alternative to many of these shortcomings and have thus been extensively pursued for more than a decade.<sup>4,5</sup>

Recently, hydrazine solution processing has been developed as a simple and high-throughput process for the

preparation of chalcopyrite thin films for solar cell applications.<sup>6–11</sup> Though this process is still in the early stages of development, CuInSe<sub>2</sub>-based thin film solar cells with efficiencies of up to 12.8% have been demonstrated.<sup>10</sup> In this approach, Cu<sub>2</sub>S and In<sub>2</sub>Se<sub>3</sub> precursor solutions are prepared separately and then combined to form a CuInSe<sub>2</sub> precursor solution with adjustable stoichiometry. The precursor solution is then spun onto the desired substrate and forms a high quality CuIn(S,Se)<sub>2</sub> film after a thermal annealing step. This approach can also readily be used to incorporate gallium into the final films.<sup>6,7</sup>

In order to further enhance the efficiency of hydrazine solution processed chalcopyrite thin film solar cells, it will be necessary to understand the structure of the involved precursor species and their interactions within the hydrazine solutions. Previously, hydrazine precursor research has been based on information obtained from the study of solid specimens prepared by the drying of the corresponding precursor solutions.<sup>12–14</sup> However, in order to gain a better understanding of the deposition and film formation processes, it is essential to identify the molecular species as they are present in the liquid-phase hydrazine precursor solutions.

In this study, we investigate the molecular structures present in solutions containing Cu<sub>2</sub>S, In<sub>2</sub>Se<sub>3</sub>, or mixtures of the two through Raman spectroscopy. This characterization technique offers the unique opportunity to simultaneously probe the vibrational modes of a variety of solvated species and has previously been proven a valuable

\*To whom correspondence should be addressed. Mailing address: Materials Science and Engineering, University of California Los Angeles, Los Angeles, CA 90095. Phone: (310) 825-4052. Fax: (310) 825-3665. E-mail: yangy@ucla.edu.

- (1) Repins, I.; Contreras, M. A.; Egaas, B.; DeHart, C.; Scharf, J.; Perkins, C. L.; To, C.; Noufi, R. *Prog. Photovolt. Res. Appl.* **2008**, *16*, 235.
- (2) Kapur, V. K.; Bansal, A.; Le, P.; Asensio, O. I. *Thin Solid Films* **2003**, *431–432*, 53.
- (3) Kaelin, M.; Rudmann, D.; Tiwari, A. N. *Sol. Energy* **2004**, *77*, 749.
- (4) Kaelin, M.; Rudmann, D.; Kurdesau, F.; Zogg, H.; Meyer, T.; Tiwari, A. N. *Thin Solid Films* **2005**, *480–481*, 486.
- (5) Hibberd, C. J.; Chassaing, E.; Liu, W.; Mitzi, D. B.; Linco, D.; Tiwari, A. N. *Prog. Photovolt. Res. Appl.* **2010**, *18*, 434.
- (6) Mitzi, D. B.; Yuan, M.; Liu, W.; Kellock, A. J.; Chey, S. J.; Deline, V.; Schrott, A. G. *Adv. Mater.* **2008**, *20*, 3657.
- (7) Mitzi, D. B.; Yuan, M.; Liu, W.; Kellock, A. J.; Chey, S. J.; Gignac, L.; Schrott, A. G. *Thin Solid Films* **2009**, *517*, 2158.
- (8) Yuan, M.; Mitzi, D. B.; Liu, W.; Kellock, A. J.; Chey, S. J.; Deline, V. R. *Chem. Mater.* **2010**, *22*, 285.
- (9) Liu, W.; Mitzi, D. B.; Yuan, M.; Kellock, A. J.; Chey, S. J.; Gunawan, O. *Chem. Mater.* **2010**, *22*, 1010.
- (10) Todorov, T.; Mitzi, D. B. *Eur. J. Inorg. Chem.* **2010**, *2010*, 17.
- (11) Hou, W. W.; Bob, B.; Li, S.-H.; Yang, Y. *Thin Solid Films* **2009**, *517*, 6853.

- (12) Milliron, D. J.; Mitzi, D. B.; Copel, M.; Murray, C. E. *Chem. Mater.* **2006**, *18*, 587.
- (13) Mitzi, D. B. *Inorg. Chem.* **2007**, *46*, 926.
- (14) Mitzi, D. B.; Copel, M.; Chey, S. J. *Adv. Mater.* **2005**, *17*, 1285.

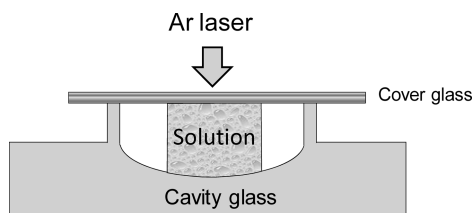


**Figure 1.** Schematic diagram for the encapsulation system used to protect the hydrazine specimens during Raman spectrum acquisition.

tool in the study of hydrazine-based systems.<sup>15</sup> We also examine the formation of the  $\text{CuIn}(\text{Se},\text{S})_2$  phase after annealing the solution-processed precursor films.

### Experimental Section

Sulfur and selenium solutions were prepared by dissolving elemental sulfur (Aldrich, 99.998%) and elemental selenium (Alfa Aesar, 99.999%) into hydrazine (Aldrich, anhydrous, 98%). In order to prepare  $\text{Cu}_2\text{S}$  solutions with controlled S/ $\text{Cu}_2\text{S}$  ratios, 1 mmol of  $\text{Cu}_2\text{S}$  (American Elements, 99.999%) was combined with an appropriate amount of elemental sulfur in 4 mL of hydrazine. To prepare  $\text{In}_2\text{Se}_3$  solutions with similarly controlled Se/ $\text{In}_2\text{Se}_3$  ratios, 1 mmol of  $\text{In}_2\text{Se}_3$  (American Elements, 99.999%) was combined with appropriate amounts of elemental selenium in 4 mL of hydrazine. The  $\text{CuIn}(\text{Se},\text{S})_2$  precursor solutions were prepared by combining a  $\text{Cu}_2\text{S}$  solution with an S/ $\text{Cu}_2\text{S}$  ratio of 0.33 with an  $\text{In}_2\text{Se}_3$  solution of Se/ $\text{In}_2\text{Se}_3$  ratio 1 in equal proportions. Solution preparation was done inside a  $\text{N}_2$  filled drybox with the oxygen and moisture levels both below 1 ppm. All solutions were stirred for more than 1 week at room temperature. *Caution: hydrazine is highly toxic and should be handled with appropriate protecting equipment to prevent contact with either the vapors or liquid.* In order to form  $\text{CuIn}(\text{Se},\text{S})_2$  thin films, the precursor solution was spun onto Mo-coated glass substrates at 3000 rpm for 50 s, followed by thermal treatment at temperatures ranging from 120 to 370 °C for 30 min.

Raman analysis was performed on the hydrazine precursor solutions and  $\text{CuIn}(\text{Se},\text{S})_2$  thin films in a backscattering configuration with a confocal configuration at room temperature with unpolarized light using a Renishaw inVia Raman system equipped with a 514.5 nm Ar laser. Laser power was adjusted to 12.5 and 1.25 mW for precursor solutions and thin films, respectively. The laser beam size was approximately 1 and 10  $\mu\text{m}$  for precursor solutions and films, respectively. The intensities of the peaks due to hydrazine in the precursor solutions were normalized to one another in order to facilitate comparison between the spectra. All curve fitting was done using Wire 3.2 software as provided by the supplier. Prior to measurement, each solution was sealed by placing vacuum grease between a cavity slide and a thin cover glass while inside an  $\text{N}_2$  filled drybox in order to reduce the possibility of chemical changes due to oxygen and moisture. A diagram of the encapsulation schematic is shown in Figure 1.

### Results and Discussion

$\text{Cu}_2\text{S}$  precursor solutions were prepared by mixing  $\text{Cu}_2\text{S}$  and elemental sulfur in hydrazine. Additionally, sulfur solutions were prepared separately, so that the bonding environment of each reactant could be analyzed

individually. The Raman spectrum of a 0.5 M sulfur solution exhibits a distinct band located at  $2560\text{ cm}^{-1}$  as shown in Figure 2a, which can be assigned to an S–H stretching vibrational mode.<sup>16</sup> Conspicuously absent from the spectrum is the S–S stretching mode, which typically appears in the range  $380\text{--}540\text{ cm}^{-1}$ , despite the fact that this mode typically produces a strong Raman signal.<sup>17</sup> Therefore, it is reasonable to assume that sulfur atoms are mainly bonded to hydrogen atoms in the form of  $\text{H}_2\text{S}$  or  $(\text{N}_2\text{H}_5)_2\text{S}$  molecules. Previous studies of the S–H stretching mode of  $\text{H}_2\text{S}$  have shown its position to typically fall at values  $20\text{--}30\text{ cm}^{-1}$  larger than the observed peak of  $2560\text{ cm}^{-1}$  shown in Figure 2a.<sup>18</sup> Thus, it is most probable that the elemental sulfur in solution has formed  $(\text{N}_2\text{H}_5)_2\text{S}$  molecules according to the following chemical reaction:<sup>19</sup>

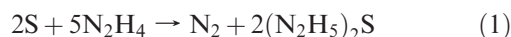


Figure 2b shows the Raman spectrum of a 0.25 M  $\text{Cu}_2\text{S}$  precursor solution in which the S/ $\text{Cu}_2\text{S}$  molar ratio has been adjusted to 2. Two distinct peaks are visible at 335 and  $2560\text{ cm}^{-1}$ , respectively. The peak located at  $335\text{ cm}^{-1}$  can be assigned to a Cu–S stretching mode,<sup>20</sup> while the peak at  $2560\text{ cm}^{-1}$  is once again the S–H stretching mode of  $(\text{N}_2\text{H}_5)_2\text{S}$  molecules formed by the elemental sulfur present in the solution. Numerical analysis shows the integrated intensity of the S–H peak in the 0.25 M  $\text{Cu}_2\text{S}$  solution spectrum to be slightly smaller than that produced by the 0.5 M sulfur solution. Since the amount of elemental sulfur added into these two solutions was originally the same, the slightly reduced S–H signal indicates that some of the elemental sulfur present has reacted with  $\text{Cu}_2\text{S}$  to form a  $\text{Cu}_x\text{S}_y$  complex which is no longer capable of exhibiting an S–H vibrational mode.

In order to identify the composition of the  $\text{Cu}_x\text{S}_y$  complex, we investigate the intensities of the S–H vibrational peak in  $\text{Cu}_2\text{S}$  precursor solutions containing a variety of S/ $\text{Cu}_2\text{S}$  molecular ratios. Figure 2c shows the intensities of the Cu–S and S–H peaks as a function of the S/ $\text{Cu}_2\text{S}$  molecular ratio. The concentration of  $\text{Cu}_2\text{S}$  was fixed to be 0.25 M, while the concentration of elemental sulfur was varied in order to adjust the S/ $\text{Cu}_2\text{S}$  ratio in the solutions. The intensity of the Cu–S peak remained constant versus the S/ $\text{Cu}_2\text{S}$  ratio, indicating that the  $\text{Cu}_2\text{S}$  powder was fully dissolved in each sample. In contrast, the intensity of the S–H peak increased linearly with the S/ $\text{Cu}_2\text{S}$  ratio and can be traced back to its  $x$ -intercept at an S/ $\text{Cu}_2\text{S}$  value of approximately 0.33. Since the  $x$ -intercept represents the point at which all added sulfur has been consumed by the  $\text{Cu}_x\text{S}_y$  complex formation

(15) Ziomek, J. S.; Zeidler, M. D. *J. Mol. Spectrosc.* **1963**, *11*, 163.

(16) Ozaki, Y.; Mizunol, T. A.; Itoh, K.; Iriyama, K. *J. Biol. Chem.* **1987**, *262*, 15445.

(17) Laitinen, R.; Steudel, R. *J. Mol. Struct.* **1980**, *68*, 19.

(18) Tang, S.-Y.; Brwon, C. W. *J. Raman Spectrosc.* **1974**, *2*, 209.

(19) Deryagina, E. N.; Levanova, E. P.; Grabel'nykh, V. A.; Sukhomazova, N.; Russavskaya, N. V.; Korchevin, N. A. *Russ. J. Gen. Chem.* **2005**, *75*, 194.

(20) Andrew, C. R.; Yeom, H.; Valentine, J. S.; Karlsson, B. G.; Bonander, N.; Pouderoyen, G.; Canters, G. W.; Loehr, T. M.; Loehr, J. S. *J. Am. Chem. Soc.* **1994**, *116*, 11489.

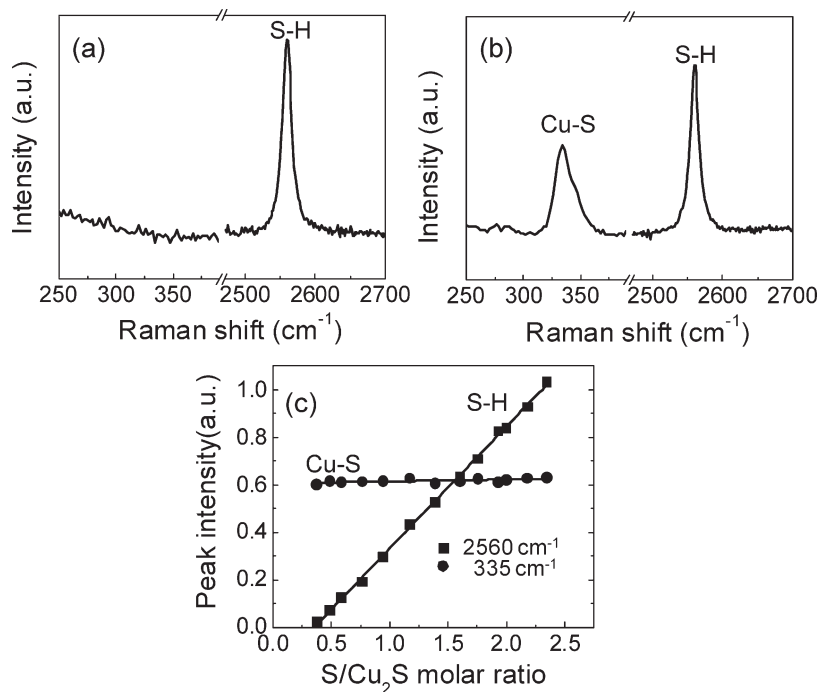
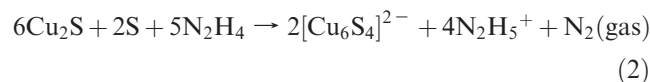


**Figure 2.** Raman spectra of (a) the 0.5 M sulfur solution and (b) the 0.25 M  $\text{Cu}_2\text{S}$  precursor solution having an S/ $\text{Cu}_2\text{S}$  ratio of 2. (c) The integrated intensities of the peaks located at 335 (●) and at 2560  $\text{cm}^{-1}$  (■) as a function of S/ $\text{Cu}_2\text{S}$  ratio obtained from the 0.25 M  $\text{Cu}_2\text{S}$  precursor solutions.

reaction, it can be concluded that the S/ $\text{Cu}_2\text{S}$  ratio of the complex is 0.33. At S/ $\text{Cu}_2\text{S}$  values smaller than 0.33, we observed black precipitates in the solution, which were assumed to be undissolved  $\text{Cu}_2\text{S}$ . From this information, we propose that  $[\text{Cu}_6\text{S}_4]^{2-}$  ions are formed by the following overall chemical reaction in hydrazine:



It has been previously reported that the  $\text{Cu}_6\text{S}_4$  anion is relatively stable and is less reactive than other  $\text{Cu}_x\text{S}_y$  complexes.<sup>21</sup> Additionally, the evaporation of  $\text{Cu}_2\text{S}$  precursor solutions has been shown to produce the compound  $\text{N}_4\text{H}_9\text{Cu}_7\text{S}_4$ , which is composed of extended  $\text{Cu}_7\text{S}_4$  sheets separated by a mixture of hydrazinium and hydrazine molecules.<sup>13</sup> Therefore, we assume that  $[\text{Cu}_6\text{S}_4]^{2-}$  ions present in a hydrazine solution convert into  $\text{Cu}_7\text{S}_4$  sheets by losing sulfur during the drying process.

Following an analogous procedure, we have also analyzed  $\text{In}_2\text{Se}_3$  precursor solutions prepared by dissolving  $\text{In}_2\text{Se}_3$  and elemental selenium in hydrazine. Figure 3a shows the Raman spectrum of a 0.1 M selenium solution. The most intense peak, located at 260  $\text{cm}^{-1}$ , can be attributed to symmetric Se–Se stretching in the  $\text{Se}_8$  cyclic species while the peak at 235  $\text{cm}^{-1}$  most likely represents Se–Se vibration in polymeric selenium chains.<sup>22,23</sup> Thus, it appears that elemental selenium dissolves in hydrazine

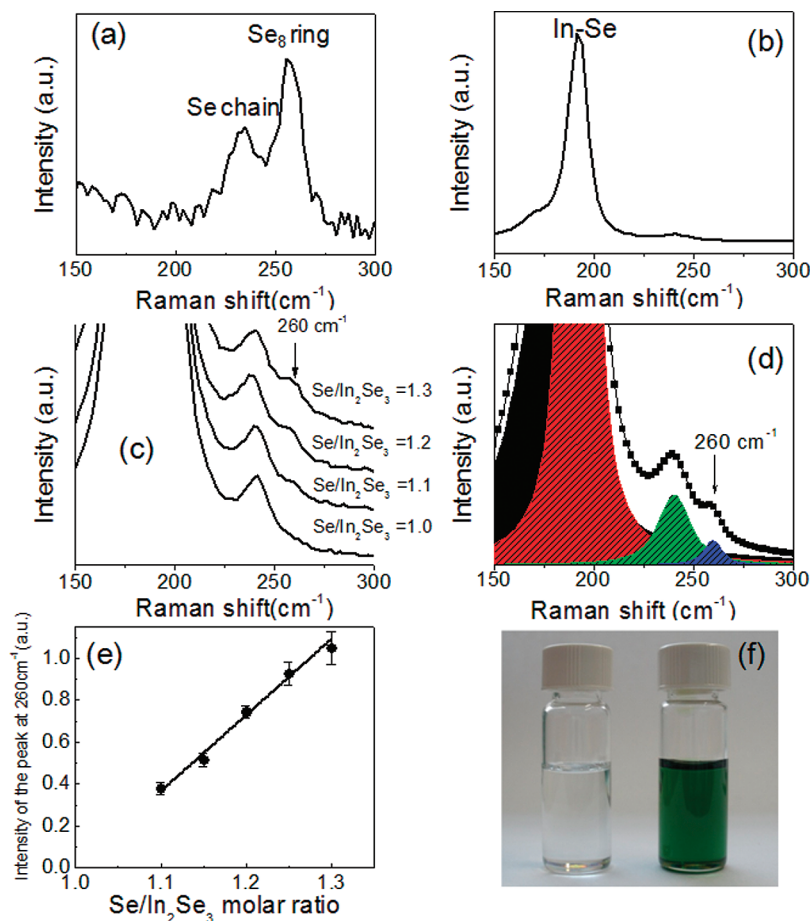
to form polyselenide molecules such as  $\text{Se}_8$  rings and polymeric chains. The observed dark green color of the elemental selenium solution supports this conclusion, since polyselenide molecules have previously been shown to produce solutions of similar colors.<sup>24</sup>

Figure 3b shows the Raman spectrum of a 0.25 M  $\text{In}_2\text{Se}_3$  precursor solution containing an equal molar amount of elemental selenium and  $\text{In}_2\text{Se}_3$ . The Raman spectrum of the solution exhibits a strong peak at 192  $\text{cm}^{-1}$  that can be attributed to the In–Se stretching mode.<sup>25</sup> The additional bands at 175 and 240  $\text{cm}^{-1}$  can be assigned to secondary vibrational modes also observed in indium selenide complexes.<sup>26–28</sup> The Se–Se stretching modes were not detected, despite the significant amount of elemental selenium that was added to the solution. This indicates that all of the elemental selenium added into the solution had been consumed during the formation of an indium selenide complex.

Figure 3c shows the Raman spectra of several Se-rich solutions, prepared with Se/ $\text{In}_2\text{Se}_3$  ratios ranging between 1 and 1.3. As shown in the figure, the Se-rich solutions show an additional peak at 260  $\text{cm}^{-1}$  that corresponds to the previously absent Se–Se stretching mode. The peaks resulting from the indium selenide complex, however, show negligible changes as the relative selenium concentration is increased. This indicates that all selenium atoms above a threshold Se/ $\text{In}_2\text{Se}_3$  ratio remain free to form polyselenide molecules, while a set amount of selenium

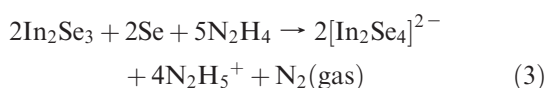
(21) Fisher, K.; Dance, I.; Willett, G.; Yi, M. *J. Chem. Soc., Dalton Trans.* **1996**, 709.  
 (22) Yannopoulos, S. N.; Andrikopoulos, K. S. *J. Chem. Phys.* **2004**, *121*, 4747.  
 (23) Nagata, K.; Ishigawa, T.; Miamoto, Y. *Jpn. J. Appl. Phys.* **1985**, *24*, 1171.

(24) Bjorgvinsson, M.; Schrobilgen, G. *J. Inorg. Chem.* **1991**, *30*, 2540.  
 (25) Dhingra, S. S.; Kanatzidis, M. G. *Inorg. Chem.* **1993**, *32*, 1350.  
 (26) Watanabe, I.; Yamamoto, T. *Jpn. J. Appl. Phys.* **1985**, *24*, 1282.  
 (27) Uhl, W.; Graupner, R.; Reuter, H. *J. Organomet. Chem.* **1996**, *523*, 227.  
 (28) Weszka, J.; Daniel, Ph.; Burian, A.; Burian, A. M.; Nguyen, A. T. *J. Non-Cryst. Solids* **2000**, *265*, 98.



**Figure 3.** Raman spectra of (a) the 0.1 M selenium solution, (b) the 0.25 M  $\text{In}_2\text{Se}_3$  precursor solution with an  $\text{Se}/\text{In}_2\text{Se}_3$  ratio of 1, and (c) several Se-rich 0.25 M  $\text{In}_2\text{Se}_3$  precursor solutions with various  $\text{Se}/\text{In}_2\text{Se}_3$  ratios. (d) Deconvolution of the peaks obtained from the  $\text{In}_2\text{Se}_3$  precursor solution with an  $\text{Se}/\text{In}_2\text{Se}_3$  ratio of 1.3. (e) The integrated intensity of the peak located at  $260\text{ cm}^{-1}$  as a function of the  $\text{Se}/\text{In}_2\text{Se}_3$  ratio in the Se-rich 0.25 M  $\text{Se}/\text{In}_2\text{Se}_3$  precursor solutions. (f) A picture of the  $\text{Se}/\text{In}_2\text{Se}_3$  precursor solutions containing an equal molar amount of elemental selenium and  $\text{In}_2\text{Se}_3$  (left) and with an  $\text{Se}/\text{In}_2\text{Se}_3$  ratio of 1.1 (right).

preferentially reacts with  $\text{In}_2\text{Se}_3$  to form indium selenide complexes. We have obtained the intensity of the Se–Se peak located at  $260\text{ cm}^{-1}$  through the deconvolution of the complete Raman spectrum, which is shown in Figure 3d. The integrated peak intensity has been plotted as a function of  $\text{Se}/\text{In}_2\text{Se}_3$  ratio, which is shown in Figure 3e. The signal increases linearly with the  $\text{Se}/\text{In}_2\text{Se}_3$  ratio and can be traced back to its  $x$ -intercept at an  $\text{Se}/\text{In}_2\text{Se}_3$  ratio of approximately unity. Since the  $x$ -intercept represents the point at which all dissolved selenium has been consumed by the complex formation reaction, it can be concluded that the  $\text{Se}/\text{In}_2\text{Se}_3$  ratio of the complex is 1. Therefore, the dominant indium–selenium phase present in hydrazine solutions must be  $[\text{In}_2\text{Se}_4]^{2-}$ , which is formed through the following overall chemical equation:



This conclusion is supported by the color of the  $\text{In}_2\text{Se}_3$  precursor solutions, which are transparent when the amount of elemental selenium present in solution is equal to or less than the amount of  $\text{In}_2\text{Se}_3$  present. Further increases in selenium concentration cause the

color of the solution to turn dark green, indicating the presence of increasing amounts of polyselenide species (Figure 3f).

In order to examine the interactions between the complex ions  $[\text{Cu}_6\text{S}_4]^{2-}$  and  $[\text{In}_2\text{Se}_4]^{2-}$  in the combined  $\text{CuIn}(\text{Se},\text{S})_2$  precursor solution,  $\text{Cu}_2\text{S}$  and  $\text{In}_2\text{Se}_3$  solutions were prepared with  $\text{S}/\text{Cu}_2\text{S}$  and  $\text{Se}/\text{In}_2\text{Se}_3$  ratios chosen to effectively eliminate the presence of  $(\text{N}_2\text{H}_5)_2\text{S}$  and polyselenide molecules. The  $\text{Cu}_2\text{S}$  solution was formed by dissolving 1 mmol of  $\text{Cu}_2\text{S}$  and 0.33 mmol of elemental sulfur in 4 mL of hydrazine and the  $\text{In}_2\text{Se}_3$  solution by combining 1 mmol of  $\text{In}_2\text{Se}_3$  with 1 mmol of elemental selenium in 4 mL of hydrazine. A  $\text{CuIn}(\text{Se},\text{S})_2$  precursor solution was prepared by combining the two solutions in equal proportions. In addition, in order to facilitate the direct comparison of scattering signal upon mixing, the unmixed  $\text{Cu}_2\text{S}$  and  $\text{In}_2\text{Se}_3$  solutions were diluted by a factor of 2 with pure hydrazine since the combined precursor solution was necessarily diluted by 2 times when the two solutions were mixed.

Figure 4 shows the Raman spectra of the diluted  $\text{Cu}_2\text{S}$  and  $\text{In}_2\text{Se}_3$  solutions as well as the  $\text{CuIn}(\text{Se},\text{S})_2$  precursor solution. Immediately noticeable is the presence of a peak located at  $315\text{ cm}^{-1}$  in the  $\text{CuIn}(\text{Se},\text{S})_2$  precursor solution,

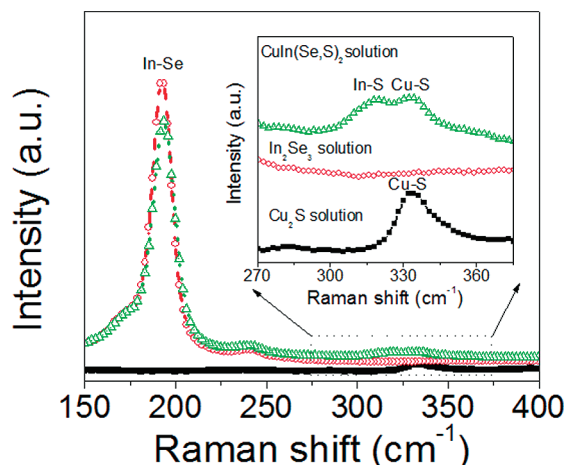


**Figure 4.** Raman spectra of the 0.125 M  $\text{Cu}_2\text{S}$  solution in which the S/ $\text{Cu}_2\text{S}$  ratio is 0.33, the 0.125 M  $\text{In}_2\text{Se}_3$  solution in which the Se/ $\text{In}_2\text{Se}_3$  ratio is unity, and the  $\text{CuIn}(\text{Se},\text{S})_2$  precursor solution prepared by mixing a 0.25 M  $\text{Cu}_2\text{S}$  solution and 0.25 M  $\text{In}_2\text{Se}_3$  solution in equal proportion.

which did not exist in the spectra of either of the individual solutions. In addition, the intensities of the In–Se and Cu–S peaks have decreased in the combined solution by approximately 15% and 25%, respectively.

According to one of the most widely used empirical relationships between bond length and force constant<sup>29,30</sup> and using information about typical Cu–S and In–S bond lengths in complex molecules,<sup>13,20,31</sup> the Cu–S and In–S force constants can be estimated to be approximately equal. The frequency of an In–S stretching mode is not readily available in the literature, but using the known Cu–S vibration frequency and approximating the two force constants as equal, we can use the harmonic oscillator approximation for isolated binary vibrational modes to estimate In–S vibration frequency:<sup>32</sup>

$$\nu(\text{In-S}) = \nu(\text{Cu-S}) \sqrt{\frac{M_{\text{Cu}}(M_{\text{In}} + M_{\text{S}})}{M_{\text{In}}(M_{\text{Cu}} + M_{\text{S}})}} \quad (4)$$

This expression produces a value for  $\nu(\text{In-S})$  of roughly  $310 \text{ cm}^{-1}$  which is very close to the value of the new Raman peak produced by the  $\text{CuIn}(\text{Se},\text{S})_2$  precursor solution as shown in the inset of Figure 4. We therefore propose the new scattering signal to result from an In–S vibrational mode. This vibration mode could be the result of anion exchange between the complex ions  $[\text{Cu}_6\text{S}_4]^{2-}$  and  $[\text{In}_2\text{Se}_4]^{2-}$  which would necessarily generate additional peaks corresponding to the Cu–Se, Se–Se, or S–H vibrational modes, which would be expected at approximately 275, 260, and  $2560 \text{ cm}^{-1}$ , respectively.<sup>33,18,22</sup> However, the creation of any other peaks besides the In–S vibration mode was not detected in the combined  $\text{CuIn}(\text{Se},\text{S})_2$  precursor solution. This suggests that the

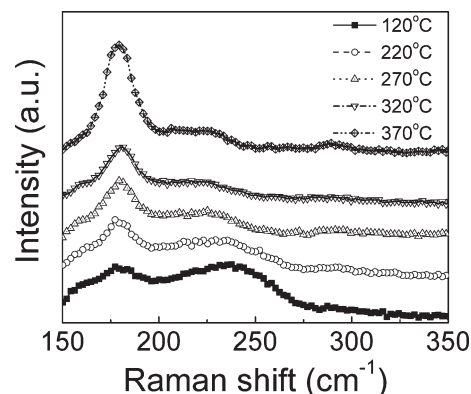


**Figure 5.** Raman spectra of several hydrazine-processed  $\text{CuIn}(\text{Se},\text{S})_2$  thin films subject to thermal annealing at temperatures ranging from 120 to 370 °C for 30 min on a hot plate in an  $\text{N}_2$ -filled drybox.

$[\text{Cu}_6\text{S}_4]^{2-}$  ions attach to the  $[\text{In}_2\text{Se}_4]^{2-}$  ions via In–S bonding in the  $\text{CuIn}(\text{Se},\text{S})_2$  precursor solution. Interaction between the two precursor species may also be responsible for the decrease of signal intensity for the In–Se and Cu–S stretching mode upon the mixing of the  $\text{Cu}_2\text{S}$  and  $\text{In}_2\text{Se}_3$  solution. It should be also noted that the In–S peak resulting from the interaction between the two species is very weak compared to the In–Se peak from  $[\text{In}_2\text{Se}_4]^{2-}$  and that the intensity of the Cu–S peak from  $[\text{Cu}_6\text{S}_4]^{2-}$  is inherently very low. Thus, it might be possible that a prospective Cu–Se peak resulting from the interaction between the two species would not be detectable over the background of the spectra. The presence of a vanishingly weak Cu–Se peak would offer the possibilities that there may be some degree of interaction between the two precursors via Cu–Se bond formation similar to the previously discussed In–S bonding or that a small amount of anion ( $\text{S}^{2-}$  or  $\text{Se}^{2-}$ ) exchange may be occurring. These possibilities should not be ruled out until further experiments can prove or disprove their validity.

The creation of In–S bonds in the  $\text{CuIn}(\text{Se},\text{S})_2$  precursor solution provides strong evidence for the mixing of copper, indium, sulfur, and selenium at a molecular level even prior to deposition. From this configuration, relatively little atomic diffusion is required to reach the chalcopyrite structure, which may make it possible to form the  $\text{CuIn}(\text{S},\text{Se})_2$  phase at fairly low temperatures. In order to explore the formation of the  $\text{CuIn}(\text{Se},\text{S})_2$  phase in deposited films, the  $\text{CuIn}(\text{Se},\text{S})_2$  precursor solution was spun onto Mo-coated soda-lime glass substrates and annealed at a range of temperatures prior to characterization. Figure 5 shows the Raman spectra of several  $\text{CuIn}(\text{Se},\text{S})_2$  thin films annealed at various temperatures.

The peak resulting from the oscillatory motion of selenium atoms with respect to their neighboring copper and indium atoms in chalcopyrite  $\text{CuInSe}_2$  is typically reported at  $174 \text{ cm}^{-1}$ .<sup>34,35</sup> The corresponding peak in our spectra is slightly shifted in energy and is located at  $178 \text{ cm}^{-1}$ , which is due to the introduction of sulfur into

(29) Badger, R. M. *J. Chem. Phys.* **1934**, *2*, 128.

(30) Herschbach, D. R. *J. Chem. Phys.* **1961**, 458.

(31) Rose, J. R.; Zubieta, J.; Fischman, A. J.; Hillier, S.; Babich, J. W. *Inorg. Chem. Commun.* **1998**, *1*, 164.

(32) Van der Ziel, J. P.; Meixner, A. E.; Kasper, H. M.; Ditzberger, J. A. *Phys. Rev. B* **1974**, *9*, 4286.

(33) Zhang, Q.-F.; Leung, W.-H.; Xin, X.-Q.; Fun, H.-K. *Inorg. Chem.* **2000**, *39*, 417.

(34) Tanino, H.; Maeda, T.; Fujikake, H.; Nakanishi, H.; Endo, S.; Irie, T. *Phys. Rev. B* **1992**, *45*, 13323.

(35) Rincon, S.; Ramirez, F. J. *J. Appl. Phys.* **1992**, *72*, 4321.

selenium sites.<sup>36</sup> The  $\text{CuIn}(\text{Se},\text{S})_2$  appears to form at as low as 120 °C. Further increase of the annealing temperature decreases the full width half-maximum of the peak at  $178\text{ cm}^{-1}$ , indicating improvement in the grain size and crystal quality of the film. The spectra show no evidence of the formation of binary phases such as CuS,  $\text{Cu}_2\text{S}$ , CuSe,  $\text{Cu}_2\text{Se}$ , and  $\text{In}_2\text{Se}_3$  which have been shown to be detrimental to photovoltaic device performance.<sup>37</sup> Compositional inhomogeneities in the precursor film can cause the formation of these binary phases at temperatures around 300 °C.<sup>38</sup> The low temperature formation of  $\text{CuIn}(\text{Se},\text{S})_2$  films free of binary phases likely results from the thorough mixing of each elemental constituent on a molecular level.

### Conclusions

In summary, elemental sulfur and selenium dissolved in hydrazine have been shown to form  $(\text{N}_2\text{H}_5)_2\text{S}$  molecules

- 
- (36) Bacewicz, R.; Gqbicki, W.; Filipowicz, J. *J. Phys.: Condens. Matter* **1994**, *6*, L777.  
(37) Alberts, V.; Zweigart, S.; Schon, J. H.; Schock, H. W.; Bucher, E. *Jpn. J. Appl. Phys.* **1997**, *36*, 5033.  
(38) Adurodija, F. O.; Song, J.; Kim, S. D.; Kwon, S. H.; Kim, S. K.; Yoon, K. H.; Ahn, B. T. *Thin Solid Films* **1999**, *338*, 13.

and polyselenide molecules such as  $\text{Se}_8$  rings and polymeric selenium chains, respectively. It has also been determined that the reaction between  $\text{Cu}_2\text{S}$  and sulfur yields  $[\text{Cu}_6\text{S}_4]^{2-}$  ions, while  $[\text{In}_2\text{Se}_4]^{2-}$  ions are formed by the reaction of  $\text{In}_2\text{Se}_3$  with selenium in hydrazine. Mixing of the  $\text{Cu}_2\text{S}$  precursor and  $\text{In}_2\text{Se}_3$  precursor solutions leads to the formation of In–S bonds, which likely bridge the two anions. This evidence suggests that all the components of the  $\text{CuIn}(\text{S},\text{Se})_2$  phase are necessarily mixed on a molecular level, which in turn enables the formation of highly uniform polycrystalline  $\text{CuIn}(\text{Se},\text{S})_2$  films at relatively low temperatures. Hydrazine solution processing therefore has tremendous potential for application to flexible solar cells, displays, and other electronics owing to the ability of this method to achieve high quality semiconductor films at low fabrication temperatures.

**Acknowledgment.** We thank Mr. D. Choi in the Department of Materials Science and Engineering of University of California, Los Angeles, for his help in the preparation of the cavity glass and Dr. Z. Chi of Renishaw Inc. for his technical assistance in the acquisition of Raman spectra.